

Saturation scale fluctuations and multi-particle rapidity correlations

Adam Bzdak¹ and Kevin Dusling²

¹*AGH University of Science and Technology,
Faculty of Physics and Applied Computer Science, 30-059 Kraków, Poland**

²*American Physical Society, 1 Research Road, Ridge, NY 11961, USA [†]*

Abstract

We study the effect of intrinsic fluctuations of the proton saturation momentum scale on event-by-event rapidity distributions. Saturation scale fluctuations generate an asymmetry in the single particle rapidity distribution in each event resulting in genuine n -particle correlations having a component linear in the rapidities of the produced particles, $y_1 \cdots y_n$. We introduce a color domain model that naturally explains the centrality dependence of the two-particle rapidity correlations recently measured by ATLAS [1] while constraining the probability distribution of saturation scale fluctuations in the proton. Predictions for $n = 4, 6$ and 8 particle correlations find that the four- and eight-particle cumulant change sign at an intermediate multiplicity, a signature which could be tested experimentally.

* bzdak@fis.agh.edu.pl

[†] kdusling@mailaps.org

I. INTRODUCTION

An outstanding challenge within the field of relativistic heavy-ion collisions is understanding the apparent collective behavior seen in smaller colliding systems ranging from p+p [2, 3], p+Pb [4–6], d+Au [7] to $^3\text{He}+\text{Au}$ [8]. For a review both on the experimental and theoretical situation we refer the reader to [9].

This is in contrast to larger system sizes, such as those produced in more-central Au+Au and Pb+Pb collisions, where a hydrodynamic treatment may be argued to be appropriate. The measured momentum-space azimuthal anisotropies, when confronted with hydrodynamic simulations, provide detailed information on the transport properties of the system and strong constraints on differing initial state treatments [10].

What remains unclear is whether the hydrodynamic paradigm is also applicable to smaller colliding systems as well. Or whether the observed anisotropies are evidence for alternative sources of collectivity, such as multi-gluon correlations already embedded in the colliding wavefunctions [11]. What is clear, is that a first principles understanding of the initial state fluctuations will be necessary to unravel the situation.

The focus of this work will be on multi-particle rapidity correlations. Just as spatial inhomogeneities in the transverse plane can be converted into azimuthal momentum-space correlation, longitudinal shape fluctuations can also be converted into momentum-space rapidity correlations [12]. This new facet can provide further insight into the nature of event-by-event fluctuations, see, e.g., [13], in particular those responsible for the highest multiplicity classes corresponding to rare configurations of the proton.

Suppose in each event the single particle rapidity distribution is asymmetric in rapidity. Statistical fluctuations could in principle generate such an asymmetry, however, these are eliminated by measuring correlation functions. Instead we will focus on dynamical fluctuations produced at the onset of the collision; for example by a disparity in the left- and right-going constituents or local fluctuations in the color charge density in the projectile and target. Regardless of the physical mechanism the event-by-event single particle distribution can be characterized by a series in rapidity,

$$\frac{dN}{dy} = \left\langle \frac{dN}{dy} \right\rangle (1 + a_0 + a_1 y + \dots) , \quad (1)$$

where $\langle dN/dy \rangle$ is the event-averaged single particle distribution. By construction we therefore have $\langle a_i \rangle = 0$ and in order to access the event-by-event fluctuations encoded in the a_i one must look at multi-particle correlations. For example, the two-particle correlation function C_2 reads [12]

$$\frac{C_2(y_1, y_2)}{\langle dN/dy_1 \rangle \langle dN/dy_2 \rangle} = \langle a_0^2 \rangle + \langle a_0 a_1 \rangle (y_1 + y_2) + \langle a_1^2 \rangle y_1 y_2 + \dots , \quad (2)$$

where

$$C_2(y_1, y_2) \equiv \left\langle \frac{d^2 N}{dy_1 dy_2} \right\rangle - \left\langle \frac{dN}{dy_1} \right\rangle \left\langle \frac{dN}{dy_2} \right\rangle . \quad (3)$$

By measuring C_2 one is able to access the root-mean-squared event-by-event fluctuations of a_i . This work will focus on the leading term $\langle a_1^2 \rangle$ (the term $\langle a_0^2 \rangle$ is related to usual multiplicity fluctuations within an event class and is of no interest to the present analysis, and $\langle a_0 a_1 \rangle = 0$ for symmetric collisions). More details can be found in [12] and [14].

In a similar fashion n -particle correlation functions, $C_n(y_1, \dots, y_n)$, closely related to the n -particle cumulants can be calculated. The correlation function $C_n(y_1, \dots, y_n)$ as defined measures genuine n -particle correlations by subtracting correlations acting between fewer than n particles. This process is described in appendix A. Here we write down the main expressions necessary for this work. The leading component of the n -particle correlation, C_n , is given by [15]

$$\frac{C_n(y_1, \dots, y_n)}{\langle dN/dy_1 \rangle \cdots \langle dN/dy_n \rangle} = \langle a_1^n \rangle_{[n]} y_1 \cdots y_n + \cdots, \quad (4)$$

where $\langle a_1^2 \rangle_{[2]} \equiv \langle a_1^2 \rangle$, as in equation 2, and

$$\langle a_1^4 \rangle_{[4]} = \langle a_1^4 \rangle - 3 \langle a_1^2 \rangle^2, \quad (5)$$

$$\langle a_1^6 \rangle_{[6]} = \langle a_1^6 \rangle - 15 \langle a_1^2 \rangle \langle a_1^4 \rangle + 30 \langle a_1^2 \rangle^3, \quad (6)$$

$$\langle a_1^8 \rangle_{[8]} = \langle a_1^8 \rangle - 28 \langle a_1^2 \rangle \langle a_1^6 \rangle - 35 \langle a_1^4 \rangle^2 + 420 \langle a_1^2 \rangle^2 \langle a_1^4 \rangle - 630 \langle a_1^2 \rangle^4. \quad (7)$$

The subscript $[n]$ denotes that the object is related to a genuine n -particle correlation. For symmetric collisions, such as p+p, the correlation function is symmetric in rapidity $C_n(y_1, \dots, y_n) = C_n(-y_1, \dots, -y_n)$ and therefore $\langle a_1^n \rangle = 0$ for $n = 1, 3, 5, \dots$.

The event-by-event fluctuations we will be interested in arise from gluon number fluctuations in the high-energy evolution of QCD. In the Color Glass Condensate framework [16] the small- x hadronic wavefunction evolves according to the B-JIMWLK [17–19] renormalization group equation. In a mean-field approximation the B-JIMWLK hierarchy reduces to a single non-linear evolution equation, the Balitsky-Kovchegov (BK) equation [20, 21]. While the BK equation serves as a good approximation to dipole evolution when the occupation number is large compared to one, it was recognized [22, 23] that that discreteness due to the finite number of partons in a given event can lead to an appreciable effect on physical observables.

A generalization of the B-JIMWLK hierarchy was derived in [24, 25] to take into account gluon number fluctuations. This hierarchy reduces (after coarse-graining in impact parameter space) to the BK equation supplemented with a stochastic noise term. The main consequence of the noise term is to introduce dispersion in the saturation scale event-by-event (as observed in numerical simulations of the Langevin BK equation [26]). The saturation scale can be treated as a random variable drawn from a probability distribution having cumulants derived in the context of a stochastic reaction diffusion model [27] which at asymptotically high energies takes the form [28],

$$P[\rho] = \frac{1}{\sqrt{2\pi}\sigma} \exp\left(-\frac{\rho^2}{2\sigma^2}\right), \quad \rho \equiv \ln\left(\frac{Q^2}{\bar{Q}^2}\right). \quad (8)$$

The variance $\sigma^2 = \alpha_s N_c / \pi D Y$ is proportional to D , the dispersion coefficient of the wavefronts, and the amount of evolution in Y . In this work we will treat σ as energy-independent parameter, fixed for LHC energies. If looking at correlations over a large range of beam energies or kinematic conditions then the evolution of σ would need to be considered.

The importance of fluctuations beyond those present in the conventional CGC framework has already been recognized. For example, in [29] fluctuations due to the impact parameter of the collision along with sub-nucleonic color charge fluctuations as implemented in the IP-Glasma model are unable to explain the tail of the multiplicity distribution in p+p collisions.

As a second example we point out that in order to obtain a quantitative description of the ridge-like correlations of high multiplicity p+p collisions the proton must fluctuate such that its effective saturation scale is 5-6 times its minimum bias value [30].

It was shown more recently that saturation scale fluctuations of the form given in equation 8 can help explain the charged particle pseudo-rapidity distributions in p+A collisions [31] and reconcile the tail of the multiplicity distribution in p+p collisions [32] finding values of $\sigma \sim 1.5$ and $\sigma \sim 0.5$ respectively.

In a previous work, reference [33], we evaluated $C_2(y_1, y_2)$ in p+p collisions from saturation scale fluctuations on an event-by-event basis drawn from the above distribution. The KLN model [34–36] for the single particle multiplicity, that has successfully accounted for the bulk multiplicity in heavy-ion collisions (see [37, 38] for recent examples at the highest LHC energies), was used to compute the asymmetric component of the two-particle correlation function for minimum bias p+p collisions. These results showed that

$$\langle a_1^2 \rangle \simeq \frac{1}{2} \lambda^2 \sigma^2 \quad (9)$$

in the limit of small σ (the full expression for any σ can be found in [33] and is rederived in section II). The parameter λ quantifies the rapidity dependence of the saturation scale due to quantum evolution

$$Q^2 = Q_o^2 e^{-\lambda y} \quad (10)$$

and has been constrained to the range $0.25 \lesssim \lambda \lesssim 0.35$ by phenomenological fits of deep inelastic scattering data at small- x [39–41]. From this constraint on λ we concluded that a value of $\sigma \sim 0.5 - 1$ is consistent with the recent ATLAS measurement [42] of $\sqrt{\langle a_1^2 \rangle} \approx 0.1$ in minimum-bias p+p collisions.

In this work we extend our study beyond two-particle correlations and find a closed form expression for the n -particle correlation function. The full result is worked out in section II but for small sigma and even n we find

$$\langle a_1^n \rangle \simeq (\lambda \sigma)^n \left[\frac{n!}{2^n (n/2)!} - \frac{n(n/2)!}{\sqrt{\pi}} \sigma + \dots \right], \quad (11)$$

and the cumulants defined in equations 5-7 can be calculated accordingly

$$\langle a_1^2 \rangle_{[2]} \simeq \frac{\lambda^2 \sigma^2}{2}, \quad \langle a_1^4 \rangle_{[4]} \simeq -\frac{2\lambda^4 \sigma^5}{\sqrt{\pi}}, \quad \langle a_1^6 \rangle_{[6]} \simeq \frac{3\lambda^6 \sigma^7}{2\sqrt{\pi}}, \quad \langle a_1^8 \rangle_{[8]} \simeq -\frac{3\lambda^8 \sigma^9}{\sqrt{\pi}}. \quad (12)$$

While the second order cumulant goes as σ^2 it is worth noting that the leading σ^n behavior of the n 'th order cumulants vanish from the subtraction of the disconnected pieces and the leading behavior becomes σ^{n+1} for $n \geq 4$.

In section III we introduce a color domain model which explains the centrality dependence of $\langle a_1^n \rangle$ through the centrality dependence of the variance, σ , of saturation scale fluctuations. In essence we argue along the same lines of [43] that correlated particle production occurs within domains of size Q_s^{-2} . The saturation scale fluctuates independently in each domain and therefore fluctuations in the impact parameter averaged (effective) saturation scale will be suppressed by the number of domains. As the multiplicity scales with the number of domains we expect that $\sigma^2 \sim 1/N_{\text{ch}}$. This argument naturally explains the ATLAS data [42] which observes that $\sqrt{\langle a_1^2 \rangle} \sim 1/N_{\text{ch}}^{0.5}$.

We should emphasize that this is not the first work to propose the use of rapidity correlations to probe the nature of the hadronic wave-function. For example, it was shown in [44, 45] that when the rapidity separation between two particles is larger than $1/\alpha_s$ the two-particle rapidity distribution is sensitive to the QCD evolution in the hadronic wave-functions of the projectile and target. For symmetric colliding systems, such as p+p or Pb+Pb, the event-averaged distribution can be asymmetric if the triggered particles have different transverse momenta. Particles of different momenta experience a differing amounts of small- x evolution and therefore decorrelate with rapidity at different speeds. However, after integrating over transverse momenta a symmetric rapidity distribution is recovered.

II. MULTI-PARTICLE CORRELATIONS

Following our previous paper [33], we will derive a general expression for the n -particle cumulant. Our starting point is the KLN expression [34–36] for single inclusive production

$$\frac{dN}{dy} \propto S_{\perp} \text{Min}[Q_1^2, Q_2^2] \left(2 + \ln \frac{\text{Max}[Q_1^2, Q_2^2]}{\text{Min}[Q_1^2, Q_2^2]} \right), \quad (13)$$

with the two saturation scales of each colliding ion represented by Q_1 and Q_2 , both of which evolve with rapidity according to

$$Q_1^2 = Q_{o,1}^2 e^{+\lambda y}, \quad Q_2^2 = Q_{o,2}^2 e^{-\lambda y}, \quad (14)$$

where $Q_{o,1}$ and $Q_{o,2}$ are the initial saturation scales at $y = 0$. The parameter λ describes the growth of the gluon structure function at small- x . It is precisely this parameter, capturing quantum corrections to the classical gluon dynamics, responsible for deviations from a purely boost-invariant (*i.e.* rapidity independent) spectra. The expression used above for the multiplicity is valid away from the fragmentation region.

The wave-function of each colliding hadron fluctuates independently on an event-by-event basis. Our goal is to study the consequence of independent fluctuations of $Q_{o,1}$ and $Q_{o,2}$ drawn from an appropriate distribution. This work will focus exclusively on the log-normal distribution motivated by studies of Langevin BK equation discussed earlier; refinements on this choice could be study for future work. Recapitulating, the saturation scale fluctuates according to the log-normal distribution,

$$P[\rho] = \frac{1}{\sqrt{2\pi}\sigma} \exp \left[-\frac{\rho^2}{2\sigma^2} \right], \quad \text{where } \rho \equiv \ln \left(\frac{Q^2}{\bar{Q}^2} \right). \quad (15)$$

The expectation value of observables are computed from

$$\langle \mathcal{O} \rangle = \int_{-\infty}^{+\infty} d\rho_1 d\rho_2 P[\rho_1] P[\rho_2] \mathcal{O}[\rho_1, \rho_2]. \quad (16)$$

For example, the mean saturation scale $\langle Q \rangle$, is related to \bar{Q} through $\langle Q \rangle = \bar{Q} \exp(\sigma^2/8)$, and therefore take $\langle Q \rangle \simeq \bar{Q}$ for $\sigma \ll 1$. In this paper we consider symmetric p+p collision and thus $\bar{Q}_{o,1}^2 = \bar{Q}_{o,2}^2 \equiv \bar{Q}_o^2$.

Defining the variables $\rho_{1,2}$ for each nucleus

$$\rho_1 \equiv \ln \frac{Q_{o,1}^2}{\bar{Q}_o^2}, \quad \rho_2 \equiv \ln \frac{Q_{o,2}^2}{\bar{Q}_o^2}, \quad (17)$$

we can re-express equation 13 as,

$$\frac{1}{S_{\perp}\bar{Q}_o^2} \frac{dN}{dy} \propto \begin{cases} e^{\rho_1+\lambda y} (2 + \rho_2 - \rho_1 - 2\lambda y), & \text{if } 2\lambda y < \rho_2 - \rho_1 \\ e^{\rho_2-\lambda y} (2 + \rho_1 - \rho_2 + 2\lambda y), & \text{if } 2\lambda y \geq \rho_2 - \rho_1 \end{cases} \quad (18)$$

The expectation value of the multiplicity can be evaluated in closed form,

$$\frac{1}{S_{\perp}\bar{Q}_o^2} \left\langle \frac{dN}{dy} \right\rangle = \frac{\sigma}{\sqrt{\pi}} \exp \left[\frac{\sigma^2}{4} - \frac{\lambda^2 y^2}{\sigma^2} \right] + \left(1 + \lambda y - \frac{\sigma^2}{2} \right) \exp \left[\frac{\sigma^2}{2} - \lambda y \right] \text{Erfc} \left[\frac{\sigma}{2} - \frac{\lambda y}{\sigma} \right] + \{y \rightarrow -y\} \quad (19)$$

where Erfc is the complementary error function. Using the above equations we can expand $\frac{dN/dy}{\langle dN/dy \rangle}$ in y , see Eq. (1), and extract the a_1 coefficient for fixed ρ_1 and ρ_2 ,

$$a_1 [\rho_1, \rho_2] = \frac{\lambda \sqrt{\pi} \exp \left(-\frac{\sigma^2}{2} \right) (\rho_1 - \rho_2) \{ \exp(\rho_1) - [\exp(\rho_1) - \exp(\rho_2)] H(\rho_1 - \rho_2) \}}{\sqrt{\pi}(\sigma^2 - 2) \text{Erfc} \left(\frac{\sigma}{2} \right) - 2\sigma \exp \left(-\frac{\sigma^2}{4} \right)} \quad (20)$$

where H is the Heaviside step function. Note that $a_1 [\rho_1, \rho_2] = 0$ for $\rho_1 = \rho_2$ since in this case there is no asymmetry. Taking the expectation value (as defined in equation 16) of the n -th power of the above expression results in,

$$\langle a_1^n \rangle = \frac{\left[\lambda \sigma \sqrt{\pi} \exp \left(\frac{\sigma^2(n-2)}{4} \right) \right]^n}{\sqrt{\pi}} \frac{n! U \left(\frac{1+n}{2}; \frac{1}{2}; \frac{n^2 \sigma^2}{4} \right)}{\left[\sqrt{\pi}(\sigma^2 - 2) \text{Erfc} \left(\frac{\sigma}{2} \right) - 2\sigma \exp \left(-\frac{\sigma^2}{4} \right) \right]^n}, \quad (21)$$

where U is the confluent hypergeometric function. Figure 1 shows $\lambda^{-1} \langle a_1^n \rangle^{1/n}$ and $\lambda^{-1} \langle a_1^n \rangle_{[n]}^{1/n}$ as a function of σ for $n = 2, 4, 6, 8$. For $\langle a_1^4 \rangle$ and $\langle a_1^8 \rangle$ the cumulant becomes negative for $\sigma \lesssim 0.5$ (independent of λ). This sign change in $\langle a_1^4 \rangle_{[4]}$ and $\langle a_1^8 \rangle_{[8]}$ is not entirely unexpected; it is a consequence of the relative strength of the intrinsic n -particle correlation from disconnected lower order contributions. A similar sign change is seen in the four-particle azimuthal cumulant which becomes negative for $N_{\text{trk}} \gtrsim 40$ [46]. In the following section we will introduce a simple color domain model relating σ^2 to the multiplicity.

III. COLOR DOMAIN MODEL

A first principle consideration of gluon number fluctuations are well beyond the scope of this work. As discussed in detail in [25, 47] extending the B-JIMWLK hierarchy to include gluon number fluctuations with impact parameter dependence results in a stochastic equation having mathematical proprieties not fully understood.

In order to make phenomenological progress, we introduce a simple model to capture the centrality dependence of σ —the variance of saturation scale fluctuations. Consider the proton in the high-energy limit of QCD at moderate value of x such that the McLerran-Venugopalan [48–50] model may serve as a good first approximation to the gluon dynamics of the nuclear wavefunction. The semi-classical small- x gluon fields are sourced by large- x valence partons treated as recoilless random color charges. The created small- x field has a correlation length $1/Q_s$, where Q_s is the typical transverse momentum of the gluons. We

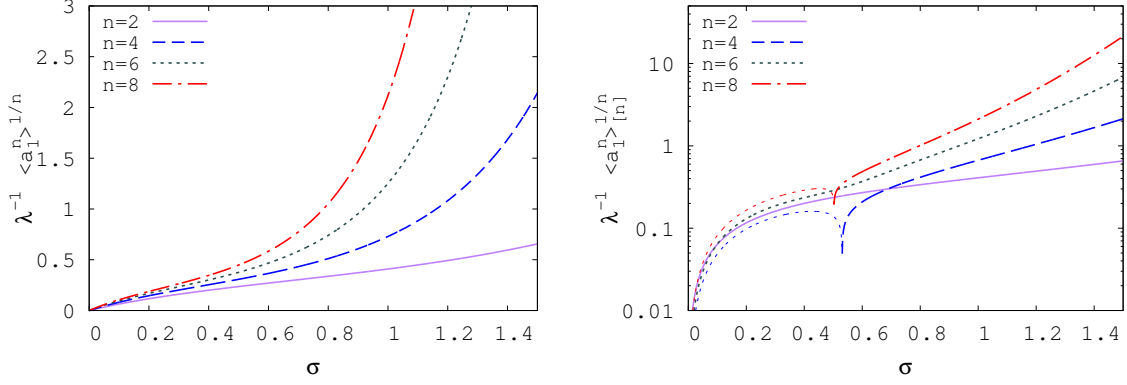


FIG. 1. Left: Equation 21 plotted as a function of σ for $n = 2, 4, 6, 8$. Right: Cumulants as defined in equations 5-7 for $n = 2, 4, 6, 8$. For $n = 4$ and $n = 8$ when the cumulant is negative ($\sigma \lesssim 0.5$) we take the absolute value and plot it as the dashed curve.

therefore assume that saturation scale fluctuations occur independently in *color domains* of size $1/Q_s$.

We picture the proton as having N_d color domains, with the saturation scale of each domain fluctuating independently according to a log-normal probability distribution of the form 8. If we identify \bar{Q}_d as the mean saturation scale of each color domain and σ_d^2 as the variance of fluctuations around the average one can generate a new probability distribution for the saturation scale fluctuations of the nucleus as a whole.

While there is no known analytic expression for the probability distribution resulting from a sum over independently fluctuating log-normal random variables it can be approximated by another log-normal [51, 52] having the following variance and mean,

$$\sigma^2 = \ln \left[\frac{1}{N_d} \left(e^{\sigma_d^2} - 1 \right) + 1 \right], \quad (22)$$

$$\ln(\bar{Q}_o^2) = \ln(\bar{Q}_d^2) + \frac{1}{4} (\sigma_d^2 - \sigma^2). \quad (23)$$

It will be instructive to look at the above result in the limit of small σ . For weak fluctuations we have $\bar{Q}_o = \bar{Q}_d$, expressing the fact that the transverse spatially averaged saturation scale is equivalent to the average saturation scale of the domains. Furthermore, for weak fluctuations the variance scales with the number of domains as

$$\sigma^2 \approx \frac{\sigma_d^2}{N_d}. \quad (24)$$

This is the expected result for a normally distributed random variable, which the log-normal approximates for small values of the variance. Given the qualitative nature of the discussion we will use the small σ approximation given in equation 24 moving forward.

It was recognized [53] that the classical fields following the collisions of two saturated nuclei consists of approximately boost-invariant longitudinal chromo-electric and -magnetic fields of transverse size Q_s^{-2} . Each flux tube emits approximately $1/\alpha_s$ gluons. A collision having overlap area S_\perp therefore has $N_{ft} \equiv (S_\perp Q_s^2)$ fluxtubes and a total multiplicity, $N_{ch} \sim 1/\alpha_s (S_\perp Q_s^2)$. Under the reasonable assumption that the number of fluxtubes scales with the

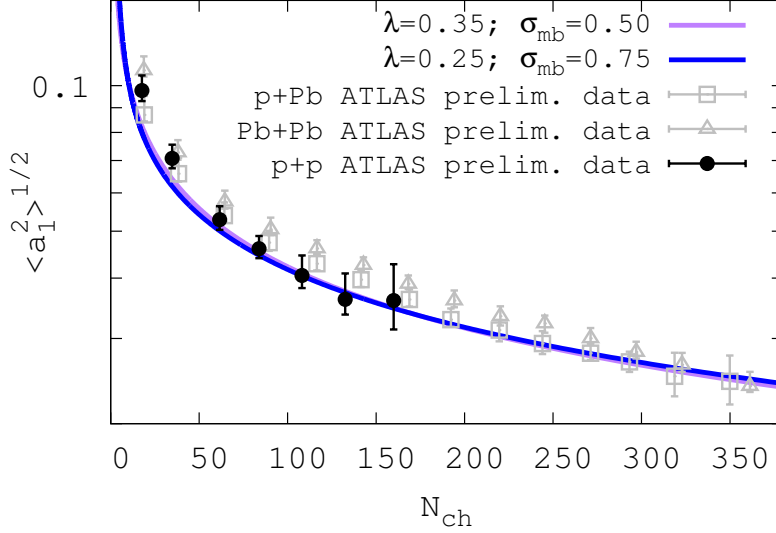


FIG. 2. $\langle a_1^2 \rangle^{1/2}$ as a function of N_{ch} compared to preliminary data in p+p collisions by the ATLAS collaboration [42]. For comparison we also show the preliminary data in p+Pb and Pb+Pb interactions.

number of color domains in the nucleus $N_{\text{ft}} \sim N_d$ we see that correlated particle production occurs within a flux tube and the correlation strength is suppressed by $1/N_{\text{ft}}$, similar in spirit to the flux-tube interpretation of the near-side ridge put forth in [43].

Based on the above considerations we can express the multiplicity dependence of σ to its value in minimum bias (mb) collisions through

$$\sigma^2 = \frac{N_{\text{ch}}^{\text{mb}}}{N_{\text{ch}}} \sigma_{\text{mb}}^2. \quad (25)$$

where $N_{\text{ch}}^{\text{mb}}$ is the minimum bias charged particle multiplicity.

We will study two values of $\lambda = 0.25$ and 0.35 covering the allowed range in phenomenological fits of Deep Inelastic Scattering data at small- x [39–41]. In figure 2 we show the centrality dependence of $\sqrt{\langle a_1^2 \rangle}$ computed from equation 21 where σ is a function of the charged particle multiplicity N_{ch} through equation 25 where we use the ATLAS value of $N_{\text{ch}}^{\text{mb}} = 17.6$. The minimum bias variance, σ_{mb} is fit to the minimum bias data as done in our previous work [33]. The agreement with data is rather striking given the single parameter fit. The parameter λ is tightly constrained by both numerical simulations of QCD evolution and phenomenological fits to data. The free parameter σ_{mb} could in principle have taken on any value but happens to fall in the range of the other approaches constraining it [31, 32]. While one could argue that the $N_{\text{ch}}^{1/2}$ dependence of the data could have fallen out of any independent cluster model, see, e.g., [13], the overall strength of the correlation is sensitive to the specific physics input that generates the correlation.

The similarity between the p+p, p+Pb and Pb+Pb experimental data may be suggestive of a similar underlying particle production mechanism, however there is no reason apriori to expect them to agree at this level. In p+Pb and Pb+Pb collisions one expects nucleonic fluctuations to have a sizable effect as shown for example in [54].

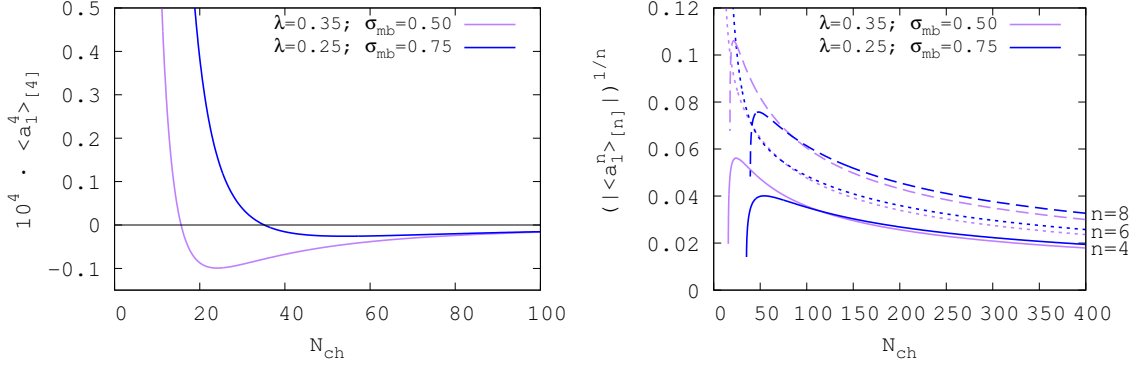


FIG. 3. Left: $10^4 \langle a_1^4 \rangle_{[4]}$ as a function of charged particle multiplicity, N_{ch} . Right: $1/\sqrt[4]{-\langle a_1^4 \rangle_{[4]}}$, $1/\sqrt[6]{\langle a_1^6 \rangle_{[6]}}$, $1/\sqrt[8]{-\langle a_1^8 \rangle_{[8]}}$ as a function of charged particle multiplicity, N_{ch} .

Figure 3 shows predictions for the higher order cumulants as a function of N_{ch} . In the left plot we show $10^4 \langle a_1^4 \rangle_{[4]}$ as a function of N_{ch} for the same parameters successfully able to reproduce the two-particle correlation. At low multiplicity the cumulant is dominated by the intrinsic four-particle correlation while at higher multiplicity lower order intrinsic correlations dominate in the subtraction specified in equation 5 making the cumulant negative.

In the right plot we present $1/\sqrt[4]{-\langle a_1^4 \rangle_{[4]}}$, $1/\sqrt[6]{\langle a_1^6 \rangle_{[6]}}$, $1/\sqrt[8]{-\langle a_1^8 \rangle_{[8]}}$ at higher multiplicity where the above quantities are real. For large multiplicities, where σ is small, we have the following analytic expressions,

$$1/\sqrt[n]{|\langle a_1^n \rangle_{[n]}|} \approx \lambda \left(\sigma_{\text{mb}}^2 \frac{N_{\text{ch}}^{\text{mb}}}{N_{\text{ch}}} \right)^{\frac{n+1}{2n}}, \quad (26)$$

for the $n = 4, 6, 8$ cumulant. A measurement of the above quantity could tightly constraint the nature of the fluctuations used in this model.

IV. CONCLUSIONS

In conclusion, we calculated and discussed multi-particle correlation functions in rapidity originating from the fluctuating saturation scales in proton-proton collisions.

The difference between the left- and right-going proton saturation scales on an event-by-event basis naturally lead to a rapidity asymmetry and consequently nontrivial long-range rapidity correlations. We focused on the first non-trivial asymmetric component, $\langle a_1^n \rangle_{[n]} y_1 \cdots y_n$ and provided compact analytical expression for the cumulants $\langle a_1^n \rangle_{[n]}$.

Introducing a simple color domain model we argued that the variance, σ , of saturation scale fluctuations is suppressed at higher multiplicities as $\sigma \sim N_{\text{ch}}^{-0.5}$, a consequence that higher multiplicity collisions necessarily contain a larger number of independently fluctuating domains.

We found a satisfactory agreement between the experimentally measured $\langle a_1^2 \rangle$ and our model and made predictions for higher order cumulants. At high multiplicities we find that the quantities $\langle a_1^4 \rangle_{[4]}$ and $\langle a_1^8 \rangle_{[8]}$ change sign to negative values; a feature which could be tested in future experiments.

We hope that this work will spur future investigations in this direction. Studying the partonic structure and accessing the Wigner distribution of the proton has been the impetus for many deep inelastic scattering experiments but have mostly been limited to a *minimum bias* proton. The experimental study of proton fluctuations has been largely limited. See [55] for a recent proposal to access these type of fluctuations in incoherent diffraction processes. Our work provides another route to access information on the proton's structure in ultra-rare configurations.

Acknowledgments:

AB was supported by the Ministry of Science and Higher Education (MNiSW), by founding from the Foundation for Polish Science, and by the National Science Centre, Grant No. DEC-2014/15/B/ST2/00175, and in part by DEC-2013/09/B/ST2/00497.

-
- [1] M. Aaboud *et al.* (ATLAS), (2016), arXiv:1606.08170 [hep-ex].
 - [2] V. Khachatryan *et al.* (CMS), Phys. Rev. Lett. **116**, 172302 (2016), arXiv:1510.03068 [nucl-ex].
 - [3] G. Aad *et al.* (ATLAS), Phys. Rev. Lett. **116**, 172301 (2016), arXiv:1509.04776 [hep-ex].
 - [4] G. Aad *et al.* (ATLAS Collaboration), Phys.Rev.Lett. **110**, 182302 (2013), arXiv:1212.5198 [hep-ex].
 - [5] B. Abelev *et al.* (ALICE Collaboration), Phys.Lett. **B719**, 29 (2013), arXiv:1212.2001 [nucl-ex].
 - [6] S. Chatrchyan *et al.* (CMS Collaboration), Phys.Lett. **B718**, 795 (2013), arXiv:1210.5482 [nucl-ex].
 - [7] A. Adare *et al.* (PHENIX), Phys. Rev. Lett. **114**, 192301 (2015), arXiv:1404.7461 [nucl-ex].
 - [8] A. Adare *et al.* (PHENIX), Phys. Rev. Lett. **115**, 142301 (2015), arXiv:1507.06273 [nucl-ex].
 - [9] K. Dusling, W. Li, and B. Schenke, Int. J. Mod. Phys. **E25**, 1630002 (2016), arXiv:1509.07939 [nucl-ex].
 - [10] U. Heinz and R. Snellings, Ann. Rev. Nucl. Part. Sci. **63**, 123 (2013), arXiv:1301.2826 [nucl-th].
 - [11] A. Dumitru, K. Dusling, F. Gelis, J. Jalilian-Marian, T. Lappi, *et al.*, Phys.Lett. **B697**, 21 (2011), arXiv:1009.5295 [hep-ph].
 - [12] A. Bzdak and D. Teaney, Phys. Rev. **C87**, 024906 (2013), arXiv:1210.1965 [nucl-th].
 - [13] W. Broniowski and P. Bozek, Phys. Rev. **C93**, 064910 (2016), arXiv:1512.01945 [nucl-th].
 - [14] J. Jia, S. Radhakrishnan, and M. Zhou, Phys. Rev. **C93**, 044905 (2016), arXiv:1506.03496 [nucl-th].
 - [15] A. Bzdak and P. Bozek, Phys. Rev. **C93**, 024903 (2016), arXiv:1509.02967 [hep-ph].
 - [16] F. Gelis, E. Iancu, J. Jalilian-Marian, and R. Venugopalan, Ann.Rev.Nucl.Part.Sci. **60**, 463 (2010), arXiv:1002.0333 [hep-ph].
 - [17] E. Iancu, A. Leonidov, and L. D. McLerran, Nucl. Phys. **A692**, 583 (2001), arXiv:hep-ph/0011241 [hep-ph].
 - [18] J. Jalilian-Marian, A. Kovner, A. Leonidov, and H. Weigert, Nucl. Phys. **B504**, 415 (1997), arXiv:hep-ph/9701284 [hep-ph].
 - [19] J. Jalilian-Marian, A. Kovner, A. Leonidov, and H. Weigert, Phys. Rev. **D59**, 014014 (1998), arXiv:hep-ph/9706377 [hep-ph].

- [20] Y. V. Kovchegov, Phys. Rev. **D61**, 074018 (2000), arXiv:hep-ph/9905214 [hep-ph].
- [21] I. Balitsky, Nucl. Phys. **B463**, 99 (1996), arXiv:hep-ph/9509348 [hep-ph].
- [22] A. H. Mueller and A. I. Shoshi, Nucl. Phys. **B692**, 175 (2004), arXiv:hep-ph/0402193 [hep-ph].
- [23] E. Iancu, A. H. Mueller, and S. Munier, Phys. Lett. **B606**, 342 (2005), arXiv:hep-ph/0410018 [hep-ph].
- [24] E. Iancu and D. N. Triantafyllopoulos, Nucl. Phys. **A756**, 419 (2005), arXiv:hep-ph/0411405 [hep-ph].
- [25] E. Iancu and D. N. Triantafyllopoulos, Phys. Lett. **B610**, 253 (2005), arXiv:hep-ph/0501193 [hep-ph].
- [26] G. Soyez, Phys. Rev. **D72**, 016007 (2005), arXiv:hep-ph/0504129 [hep-ph].
- [27] E. Brunet, B. Derrida, A. H. Mueller, and S. Munier, Phys. Rev. **E73**, 056126 (2006), arXiv:cond-mat/0512021 [cond-mat].
- [28] C. Marquet, G. Soyez, and B.-W. Xiao, Phys. Lett. **B639**, 635 (2006), arXiv:hep-ph/0606233 [hep-ph].
- [29] B. Schenke, P. Tribedy, and R. Venugopalan, Phys. Rev. **C89**, 024901 (2014), arXiv:1311.3636 [hep-ph].
- [30] K. Dusling, P. Tribedy, and R. Venugopalan, Phys. Rev. **D93**, 014034 (2016), arXiv:1509.04410 [hep-ph].
- [31] L. McLerran and M. Praszalowicz, Annals Phys. **372**, 215 (2016), arXiv:1507.05976 [hep-ph].
- [32] L. McLerran and P. Tribedy, Nucl. Phys. **A945**, 216 (2016), arXiv:1508.03292 [hep-ph].
- [33] A. Bzdak and K. Dusling, Phys. Rev. **C93**, 031901 (2016), arXiv:1511.03620 [hep-ph].
- [34] D. Kharzeev and E. Levin, Phys. Lett. **B523**, 79 (2001), arXiv:nucl-th/0108006 [nucl-th].
- [35] D. Kharzeev, E. Levin, and M. Nardi, Phys. Rev. **C71**, 054903 (2005), arXiv:hep-ph/0111315 [hep-ph].
- [36] D. Kharzeev and M. Nardi, Phys. Lett. **B507**, 121 (2001), arXiv:nucl-th/0012025 [nucl-th].
- [37] B. Abelev *et al.* (ALICE), Phys. Rev. Lett. **110**, 032301 (2013), arXiv:1210.3615 [nucl-ex].
- [38] J. Adam *et al.* (ALICE), Phys. Rev. Lett. **116**, 222302 (2016), arXiv:1512.06104 [nucl-ex].
- [39] K. J. Golec-Biernat and M. Wusthoff, Phys. Rev. **D59**, 014017 (1998), arXiv:hep-ph/9807513 [hep-ph].
- [40] M. Praszalowicz and T. Stebel, JHEP **03**, 090 (2013), arXiv:1211.5305 [hep-ph].
- [41] M. Praszalowicz and A. Francuz, Phys. Rev. **D92**, 074036 (2015), arXiv:1507.08186 [hep-ph].
- [42] The ATLAS collaboration, ATLAS-CONF-2015-051 (2015).
- [43] A. Dumitru, F. Gelis, L. McLerran, and R. Venugopalan, Nucl. Phys. **A810**, 91 (2008), arXiv:0804.3858 [hep-ph].
- [44] F. Gelis, T. Lappi, and R. Venugopalan, Phys. Rev. **D79**, 094017 (2009), arXiv:0810.4829 [hep-ph].
- [45] K. Dusling, F. Gelis, T. Lappi, and R. Venugopalan, Nucl. Phys. **A836**, 159 (2010), arXiv:0911.2720 [hep-ph].
- [46] V. Khachatryan *et al.* (CMS), Phys. Rev. Lett. **115**, 012301 (2015), arXiv:1502.05382 [nucl-ex].
- [47] A. H. Mueller, A. I. Shoshi, and S. M. H. Wong, Nucl. Phys. **B715**, 440 (2005), arXiv:hep-ph/0501088 [hep-ph].
- [48] L. D. McLerran and R. Venugopalan, Phys. Rev. **D49**, 2233 (1994), arXiv:hep-ph/9309289 [hep-ph].
- [49] L. D. McLerran and R. Venugopalan, Phys. Rev. **D49**, 3352 (1994), arXiv:hep-ph/9311205 [hep-ph].
- [50] L. D. McLerran and R. Venugopalan, Phys. Rev. **D50**, 2225 (1994), arXiv:hep-ph/9402335

[hep-ph].

- [51] L. Fenton, IRE Transactions on Communications Systems **8**, 57 (1960).
- [52] B. R. Cobb, R. Rumi, and A. Salmerón, Statistics and Computing **16**, 293 (2012).
- [53] T. Lappi and L. McLerran, Nucl. Phys. **A772**, 200 (2006), arXiv:hep-ph/0602189 [hep-ph].
- [54] B. Schenke and S. Schlichting, (2016), arXiv:1605.07158 [hep-ph].
- [55] H. Mäntysaari and B. Schenke, (2016), arXiv:1603.04349 [hep-ph].
- [56] R. Botet and M. Ploszajczak, *Universal fluctuations: The phenomenology of hadronic matter* (2002).

Appendix A: Cumulants

By definition the genuine n -particle correlation function, $C_n(y_1, \dots, y_n)$, also known as the n -particle cumulant, is different than zero only if there is an explicit correlation between n or more particles. For example, for three particles we have

$$C_3(y_1, y_2, y_3) = \left\langle \frac{d^3 N}{dy_1 dy_2 dy_3} \right\rangle - \left\langle \frac{dN}{dy_1} \right\rangle \left\langle \frac{dN}{dy_2} \right\rangle \left\langle \frac{dN}{dy_3} \right\rangle - \left\langle \frac{dN}{dy_1} \right\rangle C_2(y_2, y_3) - \left\langle \frac{dN}{dy_2} \right\rangle C_2(y_1, y_3) - \left\langle \frac{dN}{dy_3} \right\rangle C_2(y_1, y_2), \quad (\text{A1})$$

where C_2 is the two-particle correlation function, equation 3. For four particles the formula is a bit more complex

$$C_4 = \left\langle \frac{d^4 N}{dy_1 dy_2 dy_3 dy_4} \right\rangle - \left\langle \frac{dN}{dy_1} \right\rangle \left\langle \frac{dN}{dy_2} \right\rangle \left\langle \frac{dN}{dy_3} \right\rangle \left\langle \frac{dN}{dy_4} \right\rangle - \underbrace{\left\langle \frac{dN}{dy_i} \right\rangle \left\langle \frac{dN}{dy_j} \right\rangle C_2(y_k, y_l)}_6 - \underbrace{\left\langle \frac{dN}{dy_i} \right\rangle C_3(y_j, y_k, y_l)}_4 - \underbrace{C_2(y_i, y_j) C_2(y_k, y_l)}_3, \quad (\text{A2})$$

where the numbered braces show the number of possible variations. The explicit expressions for up to six particles can be found in [15] and the general formula for an arbitrary number of particles in [56].

The n -particle densities, $\left\langle \frac{d^n N}{dy_1 \dots dy_n} \right\rangle$ can be readily expressed through the $\langle a_1^k \rangle$ terms, for example

$$\begin{aligned} \frac{\left\langle \frac{d^4 N}{dy_1 \dots dy_4} \right\rangle}{\left\langle \frac{dN}{dy_1} \right\rangle \dots \left\langle \frac{dN}{dy_4} \right\rangle} &= \langle (1 + a_1 y_1) (1 + a_1 y_2) (1 + a_1 y_3) (1 + a_1 y_4) \rangle \\ &= 1 + \langle a_1^2 \rangle (y_1 y_2 + \dots + y_3 y_4) + \langle a_1^4 \rangle y_1 y_2 y_3 y_4, \end{aligned} \quad (\text{A3})$$

where for clarity we keep only the a_1 term and take $\langle a_1 \rangle = \langle a_1^3 \rangle = 0$. The genuine n -particle correlation function can be expressed by the $\langle a_1^k \rangle$ terms. For example for four particles we obtain

$$\frac{C_4(y_1, \dots, y_4)}{\langle dN/dy_1 \rangle \dots \langle dN/dy_4 \rangle} = \langle a_1^4 \rangle_{[4]} y_1 y_2 y_3 y_4 + \dots \quad (\text{A4})$$

where $\langle a_1^4 \rangle_{[4]} = \langle a_1^4 \rangle - 3 \langle a_1^2 \rangle^2$.